The Journal of Chemical Physics

Simplicity in mean-field phase behavior of two-component miktoarm star copolymers

Cite as: J. Chem. Phys. **154**, 014903 (2021); https://doi.org/10.1063/5.0037979
Submitted: 17 November 2020 . Accepted: 10 December 2020 . Published Online: 06 January 2021

Wei Li, and Yi-Xin Liu

View Online Export Citation CrossMark

© 2021 Author(s).

The Journal of Chemical Physics ARTICLE scitation.org/journal/jcp

Simplicity in mean-field phase behavior of two-component miktoarm star copolymers

Cite as: J. Chem. Phys. 154, 014903 (2021); doi: 10.1063/5.0037979
Submitted: 17 November 2020 • Accepted: 10 December 2020 •
Published Online: 6 January 2021

View Online Export Citation CrossMark

Wei Li[1,a),b)] and Yi-Xin Liu[1,2,b)]

AFFILIATIONS

[1]Materials Research Laboratory, University of California, Santa Barbara, California 93106, USA
[2]State Key Laboratory of Molecular Engineering of Polymers, Department of Macromolecular Science, Fudan University, Shanghai, China

Note: This paper is part of the JCP Emerging Investigators Special Collection.
[a)]**Present address:** Department of Chemical and Biomolecular Engineering, University of Tennessee, Knoxville, Tennessee 37996, USA.
[b)]**Authors to whom correspondence should be addressed:** wel208@mrl.ucsb.edu and lyx@fudan.edu.cn

ABSTRACT

Using self-consistent field theory, we systematically explore the microphase separation in the class of two-component miktoarm star copolymers containing a single conjunction point between different blocks by considering an extended list of candidate microphases. We plot mean-field phase diagrams in the plane of segregation strength and composition for an array of representative star copolymers. Three principal phase diagram topologies, dictated by different phase stabilities, are exposed, displaying a hierarchy in complexity by increasing the molecular asymmetry. Our investigation indicates that the phase diagram topology depends on the ratios of arm numbers and Kuhn segment lengths, which highlights the role of the coordination number ratio between different polymers at the domain interface. These findings reveal the simplicity of the general phase behavior and suggest a complete list of stable microphases for the entire class, which provide useful insight into studying copolymers with more complicated architectures and conformational properties.

Published under license by AIP Publishing. https://doi.org/10.1063/5.0037979

I. INTRODUCTION

Block copolymers, consisting of two or more chemically distinct monomers, comprise an important class of materials.[1] Due to the immiscibility between different polymer species and the constraint of chain connectivity, block copolymers can microphase separate to form ordered phase structures at mesoscale under the thermodynamic driving force, providing a unique and facile avenue to nanofabrication. The high tunability of chain architecture, chemical species, and molecular weight makes block copolymers a versatile platform for designing functional materials.[2–5] Exploring the relationship between copolymer molecular properties and phase behaviors is key for the rational design. Nevertheless, this is a daunting task for experimental studies via controlled synthesis and characterization,[6–10] while theory and simulation show distinct advantages in sweeping the related parameter space and essentially provide valuable guidance.

There have been a few theoretic attempts on exploring the effects of chain architectures on the copolymer phase behavior.[11–15] For example, de la Cruz and Sanchez[11] computed the spinodal boundaries for AB_2, A_nB_n, and $(AB)_n$ miktoarm star copolymers by using a random phase approximation (RPA),[16] which captures the variation in the stability limit of the homogeneous phase with changing copolymer architectures. Milner,[12] based on strong-stretching theory (SST),[17] compared the free energies among the classical lamellar (L), hexagonally packed cylindrical (C), and body-centered cubic spherical (S) phases, as well as an OBDD double diamond network phase, for A_mB_n stars. A molecular asymmetry parameter $\epsilon \equiv (n/m)(\rho_{0A}b_A^2/\rho_{0B}b_B^2)^{1/2}$ was derived, which combines the ratio of arm numbers (n/m), the ratio between the Kuhn segment lengths of A and B (b_A/b_B), and the density ratio (ρ_{0A}/ρ_{0B}). From SST, the minimized free energies of those phases are shown to solely depend on ϵ and copolymer composition, leading to identical phase boundaries for star copolymers of the same

Published under license by AIP Publishing

ϵ in the limit of infinite segregation strength.[12] More recently, Matsen[14] updated mean-field phase diagrams of AB diblocks and AB_2 stars and extended the calculations for $(AB)_9$ stars, infinite alternating linear, and infinite comb-like structures through self-consistent field theory (SCFT), which further implies that different copolymers sharing the same architecture units, following a decomposition principle,[6–8] have equivalent phase diagram topologies.

Despite making informative predictions, RPA and SST, invoking strict assumptions in different limits, have difficulties in probing microphases with complex structures, as well as accurately studying the practically relevant intermediate-segregation regime. By contrast, the numerical solution of SCFT offers a generic approach to investigating inhomogeneous polymeric systems with arbitrary complexity at different segregation strengths.[1,18] Since the seminal work of Matsen and Schick on using a spectral method was to solve modified diffusion equations,[19] SCFT emerges as a powerful tool for studying copolymer phase behaviors. Using SCFT, mean-field phase diagrams were constructed for various two-component block copolymers as a function of χN and f_A, where χ is the Flory–Huggins interaction parameter between A and B statistical segments, N is the degree of polymerization of the copolymer, and f_A is the volume fraction of A segments.[13,14,19–47] Meanwhile, new equilibrium microphases were predicted/examined by SCFT, including double gyroid (G),[19] closed-packed spherical (S_{cp}),[24] Fddd (O^{70}),[29] Frank–Kasper $A15$,[13,28] perforated lamellar (PL),[14] and Frank–Kasper σ[38] phases. These findings expand the repository of realizable phase structures, while calling for the revisit of relevant phase diagrams.

In this work, we employ a systematic SCFT investigation to study the microphase separation in the class of A_mB_n star copolymers containing a single conjunction point (namely, connector), which is a basic generation of two-component copolymers. The overarching goal is to present state-of-the-art phase diagrams in the χN–f_A plane for typical members (with identical A/B arms), while exploring the relationship between copolymer molecular properties and self-assembled phase structures. We inspect the effects of architecture asymmetry, $\tau_a = n/m$, and conformational asymmetry, $\tau_c = b_A/b_B$, on the phase diagram and further compare the results with the predictions from RPA and SST.[11,12,15] Our investigation, identifying key phase diagram features, serves to depict a general microphase behavior in the three-dimensional (3D) phase space by adding the molecular asymmetry as another axis to χN and f_A (see Fig. S1 of the supplementary material).

II. METHODS

We invoked an incompressible field-theoretic model of monodisperse copolymers based on continuous Gaussian chain statistics.[1,18] For simplicity, we assumed a fixed reference volume, v_0, per statistical segment and chose the volume-average segment density $\rho_{0A} = \rho_{0B} = 1/v_0$ such that $\epsilon = (n/m)(b_A/b_B) = \tau_a\tau_c$. A detailed recipe for field-theoretic models of different chain architectures can be found elsewhere.[1] SCFT calculations were performed in the real space via a pseudo-spectral method,[1] while periodic boundary conditions were enforced. A semi-implicit relaxation scheme[1] was employed for the convergence of SCFT, with an error tolerance of $10^{-7}k_BT$ per chain (k_B is the Boltzmann constant and T is the temperature) for the intensive free energy. We adopted unit-cell calculations for different microphases. For each microphase, symmetry operations in the belonging space group were applied to both auxiliary chemical potential and density fields when solving SCFT equations; the selection of the plane wave basis was optimized to saturate the intensive free energy by satisfying the error tolerance.[40] A variable cell technique[1] was utilized for the cell commensurability to obtain stress-free phase structures. In addition to the known stable phases, we included a few other microphases for the stability screening (see Fig. S2 for morphologies). Phase boundaries were located from the cross points between the free energy curves of competing stable phases.

III. RESULTS AND DISCUSSION

A. Effect of architecture asymmetry τ_a

We first examine the effect of $\tau_a = n/m$ on phase behaviors in conformationally symmetric A_mB_n stars with $b_A = b_B$. Without loss of generality, we select $m \le n$ and start with the systems of $m = 1$. Figure 1 plots the phase diagrams for AB diblocks ($\tau_a = 1$), AB_2 stars ($\tau_a = 2$), and AB_3 stars ($\tau_a = 3$), which show good agreement with previous studies.[13,14,19,30,38] The phase diagram is symmetric at $\tau_a = 1$. For $\tau_a > 1$, phase boundaries are deflected toward large f_A that skews the phase regions. Accordingly, the panel of A-rich phases on the small f_A side is enlarged, while B-rich phase regions reduce in size. Meanwhile, new complex phases emerge as τ_a increases, including σ and PL phases in AB_2 stars and an additional $A15$ phase in AB_3 stars.

The progression and connectivity of phase boundaries define the phase diagram topology. As the interfacial profile of phase domains saturates with an increase in the segregation strength χN, one would expect that the phase stabilities remain the same at large χN, while their phase boundaries become vertical as $\chi N \to \infty$ (see Ref. 30 for example). Besides the O^{70} phase regions that reside in the weak-segregation regime, the other microphase stabilities exhibit continuous progression from emergence to large χN. This simplicity of the phase diagram topology is dictated by the simplicity of the chain architecture containing a single connector, as independent connectors are anchored at the A–B interfaces and chain conformations inside phase structures are relatively simple.

In AB diblocks, the composition asymmetry, characterized by f_A, results in the spontaneous curvature at the domain interface that imparts the preference for different microphases, while the packing frustration of polymer chains inside phase structures also contributes to the microphase stability.[18,48–50] Increasing τ_a imposes an extra modification on the domain interface by affecting the ratio of polymer coordination numbers between A and B through the tethering constraint of connectors, which further adjusts the spontaneous curvature and packing frustration. This effect can be attributed as the driving force for the emergence of the new complex phases (i.e., σ, PL, and $A15$) that increases the complexity of phase diagram topologies.

As shown by Milner,[12] the free energies of the classical microphases are identical in the strong-stretching limit for star copolymers having the same ϵ, indicating a correspondence among their phase behaviors. Our SCFT calculations suggest that this correspondence exists for all the known stable microphases. Moreover,

Published under license by AIP Publishing

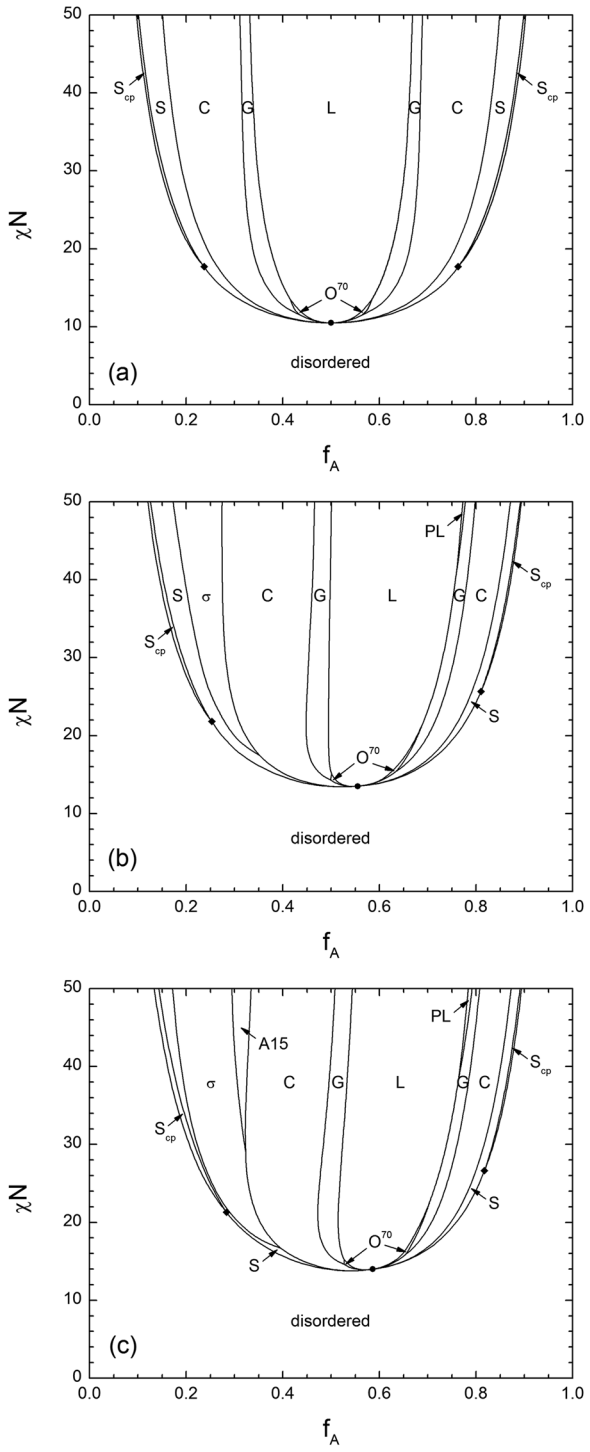

FIG. 1. Mean-field phase diagrams for (a) AB diblock, (b) AB_2 star, and (c) AB_3 star copolymers (with $b_A = b_B$, unless otherwise specified). The dot and diamonds in the phase diagram represent the critical point and triple points, respectively.[14] These phase diagrams, calculated from SCFT using a pseudo-spectral method,[1] show quantitative agreement with previous studies,[13,14,38] while the *PL* phase stability is added for AB_3 stars.

given the correspondence at large χN and the continuous progression of phase regions along with varying χN, we expect that the overall phase diagram topology should look similar for A_mB_n stars of the same τ_a, while the phase boundaries can be significantly shifted and deflected in the weak and intermediate-segregation regimes due to the difference in copolymer conformational entropies. For instance, we demonstrate the correspondence of phase stabilities between star copolymers of $m = 5$ and $m = 1$ with a focus on the spherical phase regions, where the emergence of σ and $A15$ captures the distinct differences in phase diagrams.

Figure 2 plots the phase diagram sections of A_5B_5, A_5B_{10}, and A_5B_{15} stars with respect to the rescaled segregation strength, $\chi N/m$ (with $m = 5$), while including the counterparts of $m = 1$ for comparison. A large stability region of the σ phase exists in A_5B_{10} stars; both σ and $A15$ phases are stable for A_5B_{15} stars, while they are not stable in A_5B_5 stars. The progression of phase stabilities at $m = 5$ exhibits the same sequence as $m = 1$. Comparatively, the order-disorder transition (ODT) curve of A-rich phases shifts to smaller f_A, and the ordered phase regions become wider as m increases (see complete spinodal curves[11,15] from RPA in Fig. S3). This indicates that taking A_mB_n stars as combined by m $AB_{n/m}$ stars (when n can be divided by m), the tethering constraint of the connectors reduces the polymer translational entropy and, hence, suppresses the disordered phase. Furthermore, the enlargement of σ and $A15$ phase regions implies that the preference of forming spherical Voronoi cells[38,51] in ordered phases increases with an increase in the total arm number $(m + n)$.

The correspondence of phase behaviors among copolymers with the same τ_a significantly reduces the number of phase diagram topologies for the entire class. Meanwhile, the effect of the coordination number ratio on the phase behavior appears to saturate with an increase in τ_a,[13,32] resulting in the similar phase diagrams for A_mB_n stars of the same m when $\tau_a \geq 3$ (e.g., see the example of $m = 1$ in Ref. 13). From an extensive search for stabilities of the considered competing microphases (Fig. S2), none of those phases was found stable. In consequence, only three phase diagram topologies, as exemplified by Fig. 1, have been identified from our investigation, which present the principal cases for A_mB_n stars. Moreover, two new complex phases, σ and *PL* phases, show up on the different sides of the phase diagram at $\tau_a = 2$. Our calculations suggest that these two phases emerge in tandem.

Adding τ_a as a molecular asymmetry axis to the plane of χN and f_A, the initial emergence of the corresponding triple points for σ and $A15$ phases (inside the strong-segregation regime) divides the τ_a axis into three regions; each region is associated with a group of A_mB_n stars and a particular phase diagram topology. In Fig. 3, we show the phase diagram of A_2B_3 stars to illustrate a transition state between the phase diagrams of AB diblocks and AB_2 stars. However, with the marginal stabilities of σ and *PL* phases, A_2B_3 stars share the same phase diagram topology as AB_2 stars [Fig. 1(b)]. This indicates that $\tau_a = 1.5$ belongs to the second group, while the crossover to the first group happens at $\tau_a < 1.5$ for conformationally symmetric A_mB_n stars.

B. Effect of conformational asymmetry τ_c

We next inspect the effect of $\tau_c = b_A/b_B$ on copolymer phase behaviors, with a focus on conformationally asymmetric AB diblocks for simplicity. As the free energies of the classical

Published under license by AIP Publishing

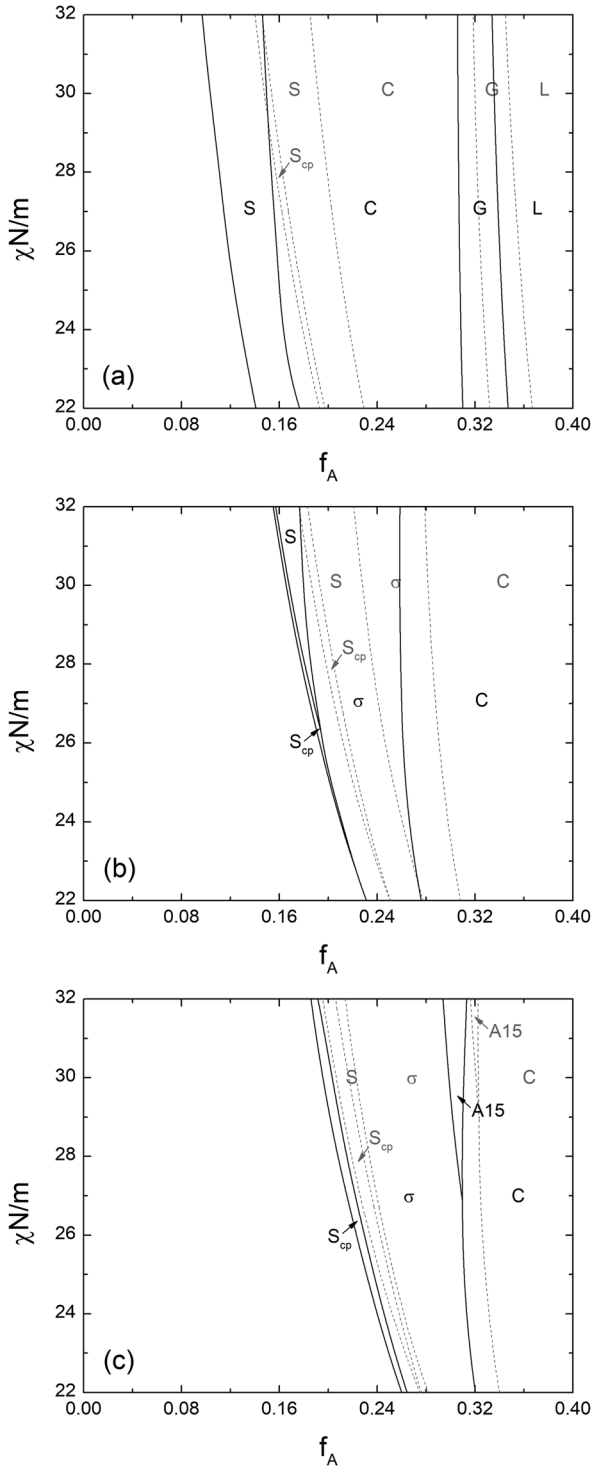

FIG. 2. Mean-field phase diagrams for (a) A_5B_5, (b) A_5B_{10}, and (c) A_5B_{15} star copolymers, focusing on the spherical phase regimes. The segregation strength is rescaled by m, which is the number of A arms in A_mB_n stars. For comparison, the corresponding phase boundaries of AB diblocks, AB_2 stars, and AB_3 stars are included in gray dashed lines.

microphases depend on $\epsilon = \tau_a\tau_c$ at infinite χN,[12] it suggests that the architecture and conformational asymmetries have similar effects and, hence, can be combined together. The correspondence between τ_a and τ_c is related to the ratio of coordination numbers between A and B segments around the domain interface. For $\tau_a = \tau_c$, effective ratios from the two asymmetries become comparable in strongly segregated phases that leads to similar chain conformations and interaction potentials between A and B (see Fig. S4 for a schematic illustration), dictating the close entropic and enthalpic contributions to free energies, respectively. Comparing the phase diagrams of conformationally asymmetric AB diblocks with A_mB_n stars at $\tau_a = \tau_c$ [e.g., $\tau_c = 1.5$ and 2.0[25,38] to A_2B_3 and AB_2 stars in Figs. 3 and 1(b)], one finds that the corresponding phase boundaries with respect to $\chi N/m$ are close in the strong-segregation regime where the effect of the coordination number ratio is dominant. In addition, the overall phase diagram morphologies are akin to each other, while the ODT curve shifts up in $\chi N/m$ for star copolymers due to the larger conformational entropy that favors the disordered phase.

Noticing the connection between τ_a and τ_c, one can refer to the conformationally symmetric A_mB_n stars of $\tau_a = \tau_c$ for the general phase behavior of AB diblocks with conformational asymmetry τ_c. According to Fig. 1, the phase boundaries are deflected toward large f_A for $\tau_c > 1$ ($b_A > b_B$), yielding larger A-rich and smaller B-rich phase regions, and vice versa. Adding τ_c as a molecular asymmetry axis, the phase diagram in the χN–f_A plane continuously evolves along τ_c in the 3D phase space (Fig. S2). From exploring the spherical phase regions, we find that the emergence of the triple point among S, σ, and C phases takes place between $\tau_c = 1.44$ and 1.45 (see Fig. S5 for free energy differences) in the strong-segregation regime. This indicates that the lower bound of the second group is below $\tau_c = 1.5$, consistent with the finding in Fig. 3 that both are for $\epsilon < 1.5$. As τ_c increases, we expect that this triple point follows a smooth curve toward smaller χN and larger f_A and eventually moves parallel to τ_c as the saturation effect develops.

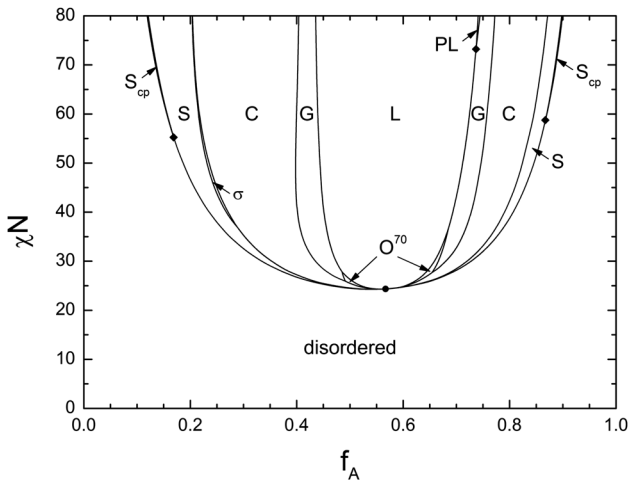

FIG. 3. Mean-field phase diagram of A_2B_3 star copolymers.

Published under license by AIP Publishing

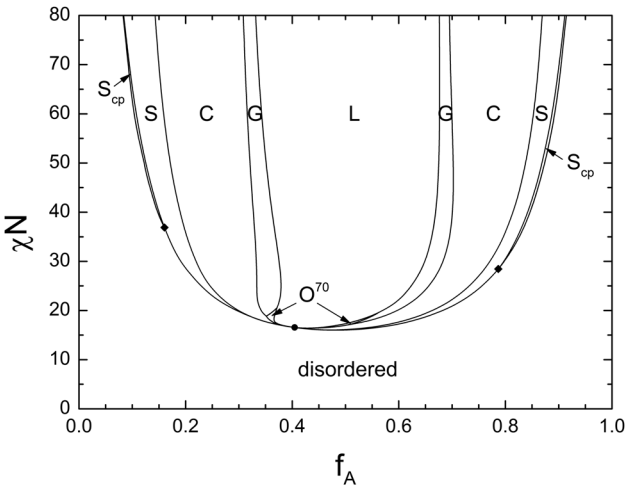

FIG. 4. Mean-field phase diagram of AB_2 star copolymers with $b_A = 1.0$ and $b_B = 2.0$ ($\tau_a = 2.0$, $\tau_c = 0.5$, and $\epsilon = 1.0$).

C. Effect of combined molecular asymmetry ϵ

After examining the individual effects of τ_a and τ_c on the phase behaviors and showing their connection, we further expose the combined effect of ϵ. Figure 4 plots the mean-field phase diagram of AB_2 star copolymers with $b_A = 1.0$ and $b_B = 2.0$ such that $\tau_a = 2$ and $\tau_c = 0.5$. As $\epsilon = 1.0$, the phase diagram has the same topology as AB diblocks [Fig. 1(a)]. At large χN, the phase boundaries are about symmetric with respect to $f_A = 0.5$ and are close to the ones of AB diblocks, implying the equivalence of phase behaviors in the strong-stretching limit. In contrast to Fig. 1(b), the critical point shifts toward small f_A on the ODT curve that correspondingly deflects the phase boundaries in the weak-segregation regime, a characteristic for the phase diagram morphology dictated by $b_A < b_B$ (which is opposite to the changes induced by $\tau_a > 1$). This indicates that at small χN when the phase segregation is weak, the conformational asymmetry has a stronger effect on the copolymer phase behaviors than the architecture asymmetry. Understanding these features, a general phase diagram morphology for a given A_mB_n melt can be delineated from locating a reference system with the same ϵ and analyzing the phase boundary deflections caused by τ_a and τ_c, which also facilitates the mapping of the accurate phase diagram.

IV. CONCLUSION

In summary, we have systematically investigated the microphase separation in the class of A_mB_n star copolymers, using SCFT calculations. Based on the phase diagram features, we demonstrate the correspondences between the phase behaviors of different star copolymers according to the asymmetry properties captured by τ_a, τ_c, and ϵ. These findings extend the SST prediction in the strong-stretching limit to the known stable microphases. Three principal phase diagram topologies, showing a hierarchy in the complexity, have been identified that suggests a complete list of stable microphases for the entire class. The individual effects of architecture and conformational asymmetries on the phase diagram morphology, as well as their connection, were examined, highlighting the role of the effective ratio between coordination numbers of A and B at the domain interface. Overall, this study describes the general mean-field phase behavior for two-component miktoarm star copolymers. We hope the presented results and the exposed simplicity will provide an updated reference that adds to the comprehensive understanding of copolymer phase behaviors.

SUPPLEMENTARY MATERIAL

See the supplementary material for additional illustrations and results.

ACKNOWLEDGMENTS

This work was supported by the National Science Foundation under Award Nos. DMR-1506008 and DMREF-1332842. Y.-X.L. was partially supported by the China Scholar Council (No. 201406105018), the Shanghai Pujiang Program (No. 18PJ1401200), and the National Natural Science Foundation of China (No. 21873021). We acknowledge Glenn Fredrickson and Kris Delaney for stimulative discussions. We further acknowledge the use of computing resources from the Center for Scientific Computing at the CNSI and MRL: an NSF MRSEC (Grant No. DMR-1720256) and an NSF (Grant No. CNS-0960316) grant.

DATA AVAILABILITY

The data that support the findings of this study are available from the corresponding author upon reasonable request.

REFERENCES

[1] G. H. Fredrickson, *The Equilibrium Theory of Inhomogeneous Polymers* (Oxford University Press, New York, 2006).
[2] T. P. Lodge, "Block copolymers: Past successes and future challenges," Macromol. Chem. Phys. **204**, 265–273 (2003).
[3] I. W. Hamley, "Ordering in thin films of block copolymers: Fundamentals to potential applications," Prog. Polym. Sci. **34**, 1161–1210 (2009).
[4] H.-C. Kim, S.-M. Park, and W. D. Hinsberg, "Block copolymer based nanostructures: Materials, processes, and applications to electronics," Chem. Rev. **110**, 146–177 (2010).
[5] F. H. Schacher, P. A. Rupar, and I. Manners, "Functional block copolymers: Nanostructured materials with emerging applications," Angew. Chem., Int. Ed. **51**, 7898–7921 (2012).
[6] S. P. Gido, C. Lee, D. J. Pochan, S. Pispas, J. W. Mays, and N. Hadjichristidis, "Synthesis, characterization, and morphology of model graft copolymers with trifunctional branch points," Macromolecules **29**, 7022–7028 (1996).
[7] C. Lee, S. P. Gido, Y. Poulos, N. Hadjichristidis, N. B. Tan, S. F. Trevino, and J. W. Mays, "H-shaped double graft copolymers: Effect of molecular architecture on morphology," J. Chem. Phys. **107**, 6460–6469 (1997).
[8] C. Lee, S. P. Gido, Y. Poulos, N. Hadjichristidis, N. B. Tan, S. F. Trevino, and J. W. Mays, "π-Shaped double-graft copolymers: Effect of molecular architecture on morphology," Polymer **39**, 4631–4638 (1998).
[9] D. J. Pochan, S. P. Gido, S. Pispas, J. W. Mays, A. J. Ryan, J. P. A. Fairclough, I. W. Hamley, and N. J. Terrill, "Morphologies of microphase-separated A_2B simple graft copolymers," Macromolecules **29**, 5091–5098 (1996).
[10] C. Lee, S. P. Gido, M. Pitsikalis, J. W. Mays, N. B. Tan, S. F. Trevino, and N. Hadjichristidis, "Asymmetric single graft block copolymers: Effect of molecular architecture on morphology," Macromolecules **30**, 3732–3738 (1997).
[11] M. O. de la Cruz and I. C. Sanchez, "Theory of microphase separation in graft and star copolymers," Macromolecules **19**, 2501–2508 (1986).

Published under license by AIP Publishing

[12]S. T. Milner, "Chain architecture and asymmetry in copolymer microphases," Macromolecules **27**, 2333–2335 (1994).
[13]G. M. Grason and R. D. Kamien, "Interfaces in diblocks: A study of miktoarm star copolymers," Macromolecules **37**, 7371–7380 (2004).
[14]M. W. Matsen, "Effect of architecture on the phase behavior of AB-type block copolymer melts," Macromolecules **45**, 2161–2165 (2012).
[15]W. Shi, Y. Tateishi, W. Li, C. J. Hawker, G. H. Fredrickson, and E. J. Kramer, "Producing small domain features using miktoarm block copolymers with large interaction parameters," ACS Macro Lett. **4**, 1287–1292 (2015).
[16]L. Leibler, "Theory of microphase separation in block copolymers," Macromolecules **13**, 1602–1617 (1980).
[17]A. N. Semenov, "Contribution to the theory of microphase layering in block-copolymer melts," Sov. Phys. JETP **61**, 733–742 (1985).
[18]M. W. Matsen, "The standard Gaussian model for block copolymer melts," J. Phys.: Condens. Matter **14**, R21–R47 (2002).
[19]M. W. Matsen and M. Schick, "Stable and unstable phases of a diblock copolymer melt," Phys. Rev. Lett. **72**, 2660–2663 (1994).
[20]J. D. Vavasour and M. D. Whitmore, "Self-consistent mean field theory of the microphases of diblock copolymers," Macromolecules **25**, 5477–5486 (1992).
[21]J. D. Vavasour and M. D. Whitmore, "Self-consistent field theory of block copolymers with conformational asymmetry," Macromolecules **26**, 7070–7075 (1993).
[22]M. W. Matsen and M. Schick, "Stable and unstable phases of a linear multiblock copolymer melt," Macromolecules **27**, 7157–7163 (1994).
[23]M. W. Matsen and M. Schick, "Microphase separation in starblock copolymer melts," Macromolecules **27**, 6761–6767 (1994).
[24]M. W. Matsen and F. S. Bates, "Unifying weak- and strong-segregation block copolymer theories," Macromolecules **29**, 1091–1098 (1996).
[25]M. W. Matsen and F. S. Bates, "Conformationally asymmetric block copolymers," J. Polym. Sci., Part B: Polym. Phys. **35**, 945–952 (1997).
[26]M. W. Matsen and R. B. Thompson, "Equilibrium behavior of symmetric ABA triblock copolymer melts," J. Chem. Phys. **111**, 7139 (1999).
[27]M. W. Matsen, "Equilibrium behavior of asymmetric ABA triblock copolymer melts," J. Chem. Phys. **113**, 5539 (2000).
[28]G. M. Grason, B. A. DiDonna, and R. D. Kamien, "Geometric theory of diblock copolymer phases," Phys. Rev. Lett. **91**, 058304 (2003).
[29]C. A. Tyler and D. C. Morse, "Orthorhombic *Fddd* network in triblock and diblock copolymer melts," Phys. Rev. Lett. **94**, 208302 (2005).
[30]E. W. Cochran, C. J. Garcia-Cervera, and G. H. Fredrickson, "Stability of the gyroid phase in diblock copolymers at strong segregation," Macromolecules **39**, 2449–2451 (2006).
[31]L. Zhang, J. Lin, and S. Lin, "Effect of molecular architecture on phase behavior of graft copolymers," J. Phys. Chem. B **112**, 9720–9728 (2008).
[32]L. Wang, L. Zhang, and J. Lin, "Microphase separation in multigraft copolymer melts studied by random-phase approximation and self-consistent field theory," J. Chem. Phys. **129**, 114905 (2008).
[33]R. Jiang, Q. Jin, B. Li, D. Ding, R. A. Wickham, and A.-C. Shi, "Phase behavior of gradient copolymers," Macromolecules **41**, 5457–5465 (2008).
[34]N. A. Lynd, F. T. Oyerokun, D. L. O'Donoghue, D. L. Handlin, and G. H. Fredrickson, "Design of soft and strong thermoplastic elastomers based on nonlinear block copolymer architectures using self-consistent-field theory," Macromolecules **43**, 3479–3486 (2010).
[35]G. Zhang, Z. Fan, Y. Yang, and F. Qiu, "Phase behaviors of cyclic diblock copolymers," J. Chem. Phys. **135**, 174902 (2011).
[36]J. U. Kim, Y.-B. Yang, and W. B. Lee, "Self-consistent field theory of Gaussian ring polymers," Macromolecules **45**, 3263–3269 (2012).
[37]J. R. Brown, S. W. Sides, and L. M. Hall, "Phase behavior of tapered diblock copolymers from self-consistent field theory," ACS Macro Lett. **2**, 1105–1109 (2013).
[38]N. Xie, W. Li, F. Qiu, and A.-C. Shi, "σ phase formed in conformationally asymmetric AB-type block copolymers," ACS Macro Lett. **3**, 906–910 (2014).
[39]Y. Gao, H. Deng, W. Li, F. Qiu, and A.-C. Shi, "Formation of nonclassical ordered phases of AB-type multi-arm block copolymers," Phys. Rev. Lett. **116**, 068304 (2016).
[40]W. Li, K. T. Delaney, and G. H. Fredrickson, "Fddd network phase in ABA triblock copolymer melts," J. Polym. Sci., Part B: Polym. Phys. **54**, 1112–1117 (2016).
[41]R. K. W. Spencer and M. W. Matsen, "Domain bridging in thermoplastic elastomers of star block copolymer," Macromolecules **50**, 1681–1687 (2017).
[42]B. Zhao, W. Jiang, L. Chen, W. Li, F. Qiu, and A.-C. Shi, "Emergence and stability of a hybrid lamella-sphere structure from linear ABAB tetrablock copolymers," ACS Macro Lett. **7**, 95–99 (2018).
[43]W. Jiang, Y. Qiang, W. Li, F. Qiu, and A.-C. Shi, "Effects of chain topology on the self-assembly of AB-type block copolymers," Macromolecules **51**, 1529–1538 (2018).
[44]S. Ahn, J. K. Kim, B. Zhao, C. Duan, and W. Li, "Morphology transitions of linear $A_1B_1A_2B_2$ tetrablock copolymers at symmetric overall volume fraction," Macromolecules **51**, 4415–4421 (2018).
[45]L. Chen, Y. Qiang, and W. Li, "Tuning arm architecture leads to unusual phase behaviors in a $(BAB)_5$ star copolymer melt," Macromolecules **51**, 9890–9900 (2018).
[46]Y. Qiang, W. Li, and A.-C. Shi, "Stabilizing phases of block copolymers with gigantic spheres via designed chain architectures," ACS Macro Lett. **9**, 668–673 (2020).
[47]Q. Xie, Y. Qiang, L. Chen, Y. Xia, and W. Li, "Synergistic effect of stretched bridging block and released packing frustration leads to exotic nanostructures," ACS Macro Lett. **9**, 980–984 (2020).
[48]S. M. Gruner, "Stability of lyotropic phases with curved interfaces," J. Phys. Chem. **93**, 7562–7570 (1989).
[49]M. W. Matsen and F. S. Bates, "Origins of complex self-assembly in block copolymers," Macromolecules **29**, 7641–7644 (1996).
[50]M. W. Matsen and F. S. Bates, "Block copolymer microstructures in the intermediate-segregation regime," J. Chem. Phys. **106**, 2436 (1997).
[51]S. Lee, C. Leighton, and F. S. Bates, "Sphericity and symmetry breaking in the formation of Frank–Kasper phases from one component materials," Proc. Natl. Acad. Sci. U. S. A. **111**, 17723–17731 (2014).

Published under license by AIP Publishing